



Ratiba Fellag <sup>1,3</sup>, Mohamed Guiatni <sup>2</sup>, Mustapha Hamerlain<sup>1</sup>,  
Noura Achour<sup>3</sup>

## Robust continuous third-order finite time sliding mode controllers for exoskeleton robot

In this work, continuous third-order sliding mode controllers are presented to control a five degrees-of-freedom (5-DOF) exoskeleton robot. This latter is used in physiotherapy rehabilitation of upper extremities. The aspiration is to assist the movements of patients with severe motor limitations. The control objective is then to design adept controllers to follow desired trajectories smoothly and precisely. Accordingly, it is proposed, in this work, a class of homogeneous algorithms of sliding modes having finite-time convergence properties of the states. They provide continuous control signals and are robust regardless of non-modeled dynamics, uncertainties and external disturbances. A comparative study with a robust finite-time sliding mode controller proposed in literature is performed. Simulations are accomplished to investigate the efficacy of these algorithms and the obtained results are analyzed.

### 1. Introduction

Stroke or cerebrovascular accident is the first leading cause to partial or full loss of motor skills in the upper extremities [1]. Specialized rehabilitation treatments with physiotherapy sessions are required to recover from these motor deficiencies, which traditionally are carried out by expert physiotherapists. Recently, robotic

✉ Ratiba Fellag, email: [rfellag@cdta.dz](mailto:rfellag@cdta.dz)

<sup>1</sup>Centre de Développement des Technologies Avancées, Alger, Algérie. ORCID R.F.: 0000-0002-2905-3988; [mhamerlain@cdta.dz](mailto:mhamerlain@cdta.dz)

<sup>2</sup>Laboratoire LCS<sup>2</sup>, Ecole Militaire Polytechnique, Alger, Algérie. ORCID M.G.: 0000-0002-5899-6862, [mohamed.guiatni@gmail.com](mailto:mohamed.guiatni@gmail.com)

<sup>3</sup>Laboratoire LRPE, Université des Sciences et de la Technologie Houari Boumediene, Alger, Algérie, [noura.achour@gmail.com](mailto:noura.achour@gmail.com)



based solutions named exoskeletons were introduced in the process of rehabilitation to enhance the quality of rehabilitation for impaired people [2]. These devices provide intensive, repetitive, precise and customized therapy while guaranteeing safety of patients and reducing the work load of therapists.

Exoskeleton robots are rigid external structures that incorporate actuators allowing controlled and precise movements as well as sensors providing information on movement related to angle, speed, and acceleration. In more advanced devices, they make it possible to capture the patient's muscular electrical activity (electromyography signals EMG) or electroencephalography (EEG), related to the intention of the movement [3, 4]. These devices are placed on the body of the person (non-invasive) and are mechanically compatible with the anatomy of the affected limb [5–7]. The main objective is to allow safe movement without resistance. Depending on the rehabilitation mode, patients can actively participate in the training exercises or be passive to the robot [8], i.e., trained by the exoskeleton robot.

Designing controllers for rehabilitation exoskeletons is very challenging as it requires rigorous robust and secure motion regulation. This research focuses on the application of Sliding Mode Control (SMC) to exoskeleton control. This approach is a powerful robust strategy for controlling robotic systems with unknown dynamics and bounded disturbances. Generally, conventional first order SMC [9, 10] employs a linear sliding surface which can only achieve asymptotic stability of the system during the sliding mode phase. This scheme suffers from chattering. Afterwards, other advanced approaches were proposed, such as Terminal SMC (TSMC) and Fast TSMC which guarantee tracking error convergence to zero in finite-time using a nonlinear surface. However, these approaches have singularity problems. To overcome this problem, nonsingular TSMC (NTSMC) has been proposed in [11, 12] as well as integral (ITSMC) [13, 14] to reduce chattering.

On the other hand, a new class of higher-order sliding mode (HOSM) controllers has emerged, extending the super-twisting algorithm (STA) proposed by A. Levant to higher orders [15–18]. The STA [19–21] is one of the most promising HOSM controllers, it produces a continuous control signal that attenuates chattering but only ensures asymptotic convergence for mechanical systems of second order. Therefore, finite time stabilization methods have been incorporated with STA using homogeneity properties [22].

The key contribution of this paper concerns the exoskeleton robot control issue. A finite-time robust tracking problem for a 5-DOF upper-limb exoskeleton robot with parametric uncertainties and external disturbances is investigated in this work. Even if this topic has been examined in the literature, there is room for improvement of current controllers. Some shortcomings of existing approaches in the literature that can be cited are the use of simplified linear models instead of coupled nonlinear models. Also, some works do not consider model uncertainties, unknown external perturbations which may lead to a lack of robustness. Most of the controllers ensure asymptotic stability for the closed-loop robotic exoskele-

ton system, which means that configuration variables of joints reach the desired trajectories within an infinite time. Motivated by these issues, we suggested two robust nonlinear sliding mode control strategies for the passive rehabilitation therapy of the shoulder, elbow, and wrist joints of a 5-DOF upper limb exoskeleton. The key characteristics of the controllers are finite-time convergence, the precision of tracking, continuity of the input control, and robustness to uncertainties and disturbances.

The dynamic modeling of the considered exoskeleton robot is first introduced. Then the first scheme of the third order STA is presented to guarantee convergence of tracking errors to zero in finite-time using a nonlinear sliding surface with fractional power. The second scheme, on the other hand, does not require the design of a sliding surface and guarantees finite-time convergence and robustness. The proposed strategies will be compared with a relevant reference wherein a NTSMC scheme is developed for the same 5-DOF exoskeleton robot to ensure finite-time stability of the closed-loop system.

The rest of the paper is structured along the subsequent sections. In section 2, we present the problem statement wherein the exoskeleton system is presented and its dynamic modeling is described. In section 3, the controllers design methodology is studied. Simulation results are drawn and analyzed after that in section 4. Finally, a conclusion is given in section 5, which ends the paper.

## 2. Problem statement

In this work, two control schemes will be designed to achieve trajectory tracking of a 5-DOF exoskeleton robot. This latter is employed for the rehabilitation of upper limbs. The control approaches will be founded on the finite-time robust third-order STA and the control task is to pursue a desired trajectory smoothly as close as possible at different points of operation.

### 2.1. Description of the system

An exoskeleton robot developed to upper limb rehabilitation is a mechatronic device that is connected in a non-invasive way to the human's upper extremities. Its primary functionality is to mimic the movements of the upper limb. Depending on the degree of motor disability of the patient and the type of rehabilitation assigned by the physiotherapist, the exoskeleton robot can perform the movement or just assist the patient into performing the movement. Moreover, it can even exert some resisting forces.

The exoskeleton robot under study is the one presented in [12, 23–25]. It is depicted in Fig. 1. In Fig. 1a is illustrated the real structure which is constituted of five-degrees-of-freedom and duplicates the human upper extremity movements [23]. The five possible movements are shoulder flexion and extension, shoulder abduction and adduction, elbow flexion and extension, internal and external rotation

and finally wrist flexion and extension. At each joint of the exoskeleton robot, a servomotor is employed to drive the necessary power to the arm. Optical encoders are used to record absolute positions of each joint (Fig. 1b).

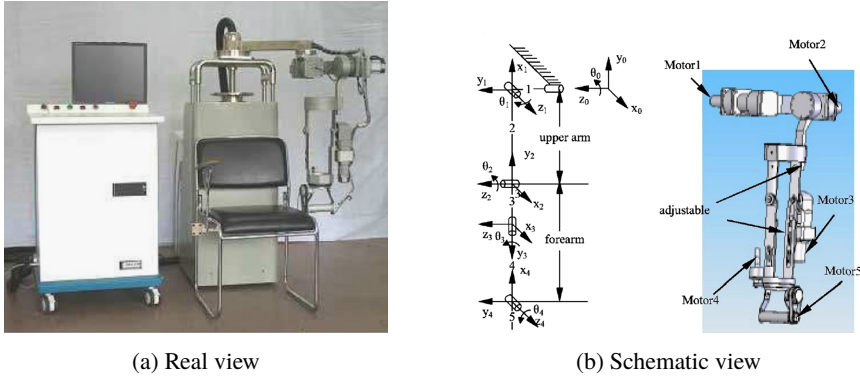


Fig. 1. Structure of the exoskeleton robot [23, 24]

## 2.2. Modeling of the system

The mathematical dynamic model for the 5-DOF exoskeleton robot is obtained using the Lagrange formalism of rigid bodies [26] in accordance with the schematic diagram of the robot depicted in Fig. 1b. It is expressed by:

$$M(q)\ddot{q} + C(q, \dot{q})\dot{q} + G(q) + F_{\text{ext}} = \tau, \quad (1)$$

whereby:  $q \in R^5$  – joint's angular positions,  $\dot{q} \in R^5$  – joint's angular velocities,  $\ddot{q} \in R^5$  – joint's angular accelerations,  $\tau \in R^5$  – actuators input torques,  $F_{\text{ext}} \in R^5$  – external disturbances assumed bounded with known bound, Matrix  $M(q) \in R^{5 \times 5}$  – inertia matrix,  $C(q, \dot{q}) \in R^{5 \times 5}$  – centrifugal forces and Coriolis matrix.  $G(q)$  – gravity vector.

The full description and the different entries of the matrices constituting the dynamic model of the exoskeleton robot can be found in [23, 24]. The variations on the joint's dynamic parameters are given by:

$$\begin{aligned} M(q) &= M_{\text{nom}}(q) + \Lambda M(q), \\ C(q, \dot{q}) &= C_{\text{nom}}(q, \dot{q}) + \Lambda C(q, \dot{q}), \\ G(q) &= G_{\text{nom}}(q) + \Lambda G(q), \end{aligned} \quad (2)$$

where  $M_{\text{nom}}(q)$ ,  $C_{\text{nom}}(q, \dot{q})$  and  $G_{\text{nom}}(q)$  describe nominal terms while uncertainties are given by  $\Lambda M(q)$ ,  $\Lambda C(q, \dot{q})$  and  $\Lambda G(q)$ .

Merging equations of (1) and (2), the dynamic model becomes:

$$M_{\text{nom}}(q)\ddot{q} + C_{\text{nom}}(q, \dot{q})\dot{q} + G_{\text{nom}}(q) = \tau(t) + \zeta(t), \quad (3)$$

with (4) a term gathering uncertainties and disturbances.

$$\zeta(t) = -\Lambda M(q)\ddot{q} - \Lambda C(q, \dot{q})\dot{q} - \Lambda G(q) - F_{\text{ext}}. \quad (4)$$

Further, rewriting (3) and (4) using state space representation with state variables  $z_1 = q$  and  $z_2 = \dot{q}$  and  $v = \tau$

$$\begin{aligned} \dot{z}_1 &= z_2, \\ \dot{z}_2 &= f(z_1, z_2, t) + g(z_1)v, \end{aligned} \quad (5)$$

wherein

$$\begin{aligned} f(z_1, z_2, t) &= M_{\text{nom}}^{-1}(z_1)(-C_{\text{nom}}(z_1, z_2) - G_{\text{nom}}(z_1) + \zeta(t)), \\ g(z_1) &= M_{\text{nom}}^{-1}(z_1). \end{aligned} \quad (6)$$

Let  $v$  be defined as in (7):

$$v = g^{-1}(z_1)u. \quad (7)$$

The closed loop system of the exoskeleton robot to be controlled is then presented as:

$$\begin{aligned} \dot{z}_1 &= z_2, \\ \dot{z}_2 &= u + f(z_1, z_2, t). \end{aligned} \quad (8)$$

**Notation:** In the following, the notation  $|\cdot|^r = |\cdot|^r \text{sign}(\cdot)$ , is used due to expressions becoming too long. Where  $r \in \mathbb{R}$ . To make it clearer, here are some examples of the new notation:

$$\lfloor y \rfloor^0 = \text{sign}(y), \quad \lfloor y \rfloor^0 y^r = |y|^r, \quad \lfloor y \rfloor^0 |y|^r = \lfloor y \rfloor^r.$$

### 3. Controllers design

In this section, two robust finite-time third-order sliding mode control algorithms are examined, which extend characteristics of second order STA, that is, they are relevant to second order systems having a relative degree of two and in addition stabilize the state variables in finite-time via a continuous control signal  $u$  such that the states of system (8) stabilize in finite-time regardless to disturbances and uncertainties  $f(z_1, z_2, t)$ .

Accordingly, to address the trajectory tracking control task applied to the upper limb exoskeleton robot, desired trajectories  $q_d$  for each joint are first proposed. They are considered twice differentiable. Therefore, the angular position tracking error vector is given by  $e_1 = q - q_d$  while its time derivative is expressed by  $e_2 = \dot{q} - \dot{q}_d$ . Consequently, the closed loop error dynamics model is expressed in (9).

$$\begin{aligned} \dot{e}_1 &= e_2, \\ \dot{e}_2 &= u + f(z_1, z_2, t) - \ddot{q}_d. \end{aligned} \quad (9)$$

**Assumption** : uncertainties and disturbances are assumed Liptchitz.

$$|\dot{f}(z_1, z_2, t)| < \Delta,$$

$\Delta$  a known bound.

### 3.1. Third order super-twisting algorithm

The second order STA algorithm proposed by A. Levant in [19] is expressed in terms of system's state variables as:

$$\begin{aligned} u_{2-sta} &= -k_1 |e_1|^{\frac{1}{2}} + L, \\ \dot{L} &= -k_3 |e_1|^0. \end{aligned} \quad (10)$$

This control algorithm generates a continuous signal, however, it establishes asymptotic convergence. This algorithm will be extended to third-order in the sequel. A nonlinear sliding surface  $\psi$  is first designed using (11)

$$\psi = e_2 + k_2 |e_1|^{\frac{2}{3}}, \quad (11)$$

where  $k_2$  is a positive gain.

Based on the previous system description (9), a robust control scheme is designed using (11) to control the upper limb rehabilitation exoskeleton robot.

**Theorem 1.** [18] The control law defined by:

$$\begin{aligned} u_{3sta} &= -k_1 |\psi|^{\frac{1}{2}} + L, \\ \dot{L} &= -k_3 |\psi|^0, \end{aligned} \quad (12)$$

where  $k_1$  and  $k_3$  are positive gains. This control law establishes robustly and in finite-time stabilization of the states of the system (9) for any disturbance  $f(z_1, z_2, t)$  that is Lipschitz with respect to time, as long as gains  $k_1$ ,  $k_2$  and  $k_3$  are appropriately designed. ■

Substituting the control law (12) into system (9):

$$\begin{aligned} \dot{e}_1 &= e_2, \\ \dot{e}_2 &= -k_1 |\psi|^{\frac{1}{2}} + L + f(z_1, z_2, t), \\ \dot{L} &= -k_3 |\psi|^0. \end{aligned} \quad (13)$$

Setting  $e_3 = L + f(z_1, z_2, t)$

$$\begin{aligned} \dot{e}_1 &= e_2, \\ \dot{e}_2 &= -k_1 |\psi|^{\frac{1}{2}} + e_3, \\ \dot{e}_3 &= -k_3 |\psi|^0 + \dot{f}(z_1, z_2, t). \end{aligned} \quad (14)$$

The system in (14) is homogeneous [27] with negative degree  $d = -1$  and the corresponding weights are  $r = [3 \ 2 \ 1]$ . Note that this algorithm coincides with the class of second order sliding mode controllers wherein only states  $z_1$  and  $z_2$  are required to stabilize in finite-time the system's states  $e_1$ ,  $e_2$  and  $e_3$  through a continuous input control signal. The main idea is to include an additional discontinuous integral term  $f(z_1, z_2, t) = \int_T^t -k_3 \lfloor \psi \rfloor^0 dt$  to cancel out the disturbance.

### 3.1.1. Necessary conditions for the convergence of the 3-STA

Considering the following candidate Lyapunov function from [18]:

$$\begin{aligned}
 V(e) = & w_1 |e_1|^{\frac{4}{3}} - w_{12} \lfloor e_1 \rfloor^{\frac{2}{3}} \psi + w_2 |\psi|^2 \\
 & + w_{13} \lfloor e_1 \rfloor^{\frac{2}{3}} \lfloor e_3 \rfloor^2 - w_{23} \psi \lfloor e_3 \rfloor^2 + w_3 |e_3|^4 .
 \end{aligned} \tag{15}$$

This Lyapunov function is homogeneous of degree 4 with weights [3 2 1]. Its time derivative is:

$$\begin{aligned}
 \dot{V}(e) = & l_1 \lfloor e_1 \rfloor^{\frac{1}{3}} e_2 - l_2 |e_1|^{-\frac{1}{3}} e_2^2 - 2k_1 w_2 |\psi|^{\frac{3}{2}} - w_{23} |e_3|^3 \\
 & - l_3 |e_1|^{-\frac{1}{3}} e_2 \lfloor e_3 \rfloor^2 + k_1 w_{12} \lfloor e_1 \rfloor^{\frac{2}{3}} \lfloor \psi \rfloor^{\frac{1}{2}} - \bar{l}_4 \lfloor e_1 \rfloor^{\frac{2}{3}} e_3 \\
 & + \bar{l}_5 e_3 \psi + w_{23} k_1 \lfloor \psi \rfloor^{\frac{1}{2}} \lfloor e_3 \rfloor^2 - \bar{l}_6 \lfloor e_3 \rfloor^3 \lfloor \psi \rfloor^0 ,
 \end{aligned} \tag{16}$$

wherein:

$$l_1 = \left( \frac{4w_1}{3} - \frac{4k_2 w_{12}}{3} + \frac{4w_2 k_2^2}{3} \right),$$

$$l_2 = \left( \frac{2w_{12}}{3} - \frac{4w_2 k_2}{3} \right),$$

$$l_3 = \left( \frac{2w_{23} k_2}{3} - \frac{2w_{13}}{3} \right),$$

$$\bar{l}_4 = \left( w_{12} + 2w_{13} k_3 \lfloor \psi \rfloor^0 \lfloor w_3 \rfloor^0 - 2w_{13} \lfloor e_3 \rfloor^0 \dot{f}(z_1, z_2, t) \right),$$

$$\bar{l}_5 = \left( w_{12} + 2w_{23} k_3 \lfloor \psi \rfloor^0 \lfloor w_3 \rfloor^0 - 2w_{23} \lfloor e_3 \rfloor^0 \dot{f}(z_1, z_2, t) \right),$$

$$\bar{l}_6 = \left( 4k_3 w_3 - 4w_3 \dot{f}(z_1, z_2, t) \lfloor \psi \rfloor^0 \right).$$

The conditions on the coefficients  $(w_1, w_{12}, w_2, w_{13}, w_{23}, w_3)$ ,  $(l_1, l_2, l_3, \bar{l}_4, \bar{l}_5, \bar{l}_6)$  and  $(k_1, k_2, k_3)$  of (14) such  $V > 0$  and  $\dot{V} < 0$  are given by:

$$\begin{aligned}
 w_1 &> 0, \\
 w_1 w_2 &> \frac{1}{4} w_{12}^2, \\
 w_1 \left( w_2 w_3 - \frac{1}{4} w_{23}^2 \right) + \frac{w_{12}}{2} \left( -\frac{w_{12} w_3}{2} + \frac{w_{13} w_{23}}{4} \right) + \frac{w_{13}}{2} \left( \frac{w_{12} w_{23}}{4} - \frac{w_2 w_{13}}{2} \right) &> 0.
 \end{aligned} \tag{17}$$

For  $\alpha_1, \alpha_2, \vartheta(\alpha_1), \vartheta(\alpha_1)$ , the following inequalities must be satisfied [28]:

$$\begin{aligned}
 l_1 k_1^2 w_{12} - k_1 w_{12} - \sqrt{\frac{2^2 \bar{l}_4^3}{3^2 (w_{23} - \bar{l}_6)}} &> \alpha_1 > 0, \\
 \vartheta &\geq \beta(\lambda, \alpha_1), \\
 \frac{2k_1^2 w_2 w_{23} - \alpha_2}{k_1^3 w_{23} w_{12}} &> \nu(\alpha_1) > 0
 \end{aligned} \tag{18}$$

and

$$\begin{aligned}
 2k_1^2 w_2 w_{23} &> \alpha_2 > 0, \\
 \vartheta(\alpha_2) &\geq \max\{\beta(\lambda_1, \alpha_2), \beta(\lambda_2, \alpha_2)\}, \\
 \frac{1}{(k_1 w_{12})^2} \left( w_{23} - |\bar{l}_6| - \frac{2^2 |\bar{l}_4|^3}{3^3 \left( l_1 k_1 - \frac{\alpha_1}{k_1 w_{12}} \right)^2} \right) &> \vartheta(\alpha_2) > 0.
 \end{aligned} \tag{19}$$

If these conditions (17), (18) and (19) are satisfied, the Lyapunov function (15) will be positive definite and its time derivative will be negative definite (16) [18, 28]. In this case,  $\dot{V}$  satisfies the differential inequalities

$$\dot{V} \leq -\kappa V^{3/4} \tag{20}$$

for some positive  $\kappa$ .

**Theorem 2.** [29]: Suppose there exists a continuous function  $V$  satisfying :

- $V$  is positive definite
- There exist real numbers  $c > 0$  and  $\kappa \in (0, 1)$  and an open neighborhood of the origin such that

$$\dot{V}(x) + c(V(x))^\kappa \leq 0,$$

then the origin is a finite-time stable equilibrium. ■

On the basis of Theorem 2, it is concluded that finite-time convergence is obtained using the 3-STA control strategy.



### 3.2. Discontinuous integral controller

The second third-order sliding mode controller extending the STA properties discussed in this work, is the discontinuous integral controller (DIC). This algorithm is stated in Theorem 3.

**Theorem 3.** [15, 16] The control law of the DIC algorithm is described by

$$\begin{aligned} u_{\text{DIC}} &= -k_1 |e_1|^{\frac{1}{3}} - k_2 |e_2|^{\frac{1}{2}} + L, \\ \dot{L} &= -k_3 |e_1|^0. \end{aligned} \quad (21)$$

This control law robustly stabilizes in finite-time the states of the system (9) for whatever disturbance  $f(z_1, z_2, t)$  having bounded time derivative for some positive gains  $k_1, k_2$  and  $k_3$ . ■

Introducing (21) into the system (9) yields the closed loop system (22):

$$\begin{aligned} \dot{e}_1 &= e_2, \\ \dot{e}_2 &= -k_1 |e_1|^{\frac{1}{3}} - k_2 |e_2|^{\frac{1}{2}} + L + f(z_1, z_2, t), \\ \dot{L} &= -k_3 |e_1|^0. \end{aligned} \quad (22)$$

Considering  $e_3 = L + f(z_1, z_2, t)$ , yields:

$$\begin{aligned} \dot{e}_1 &= e_2, \\ \dot{e}_2 &= -k_1 |e_1|^{\frac{1}{3}} - k_2 |e_2|^{\frac{1}{2}} + e_3, \\ \dot{e}_3 &= -k_3 |e_1|^0 + \dot{f}(z_1, z_2, t). \end{aligned} \quad (23)$$

It is to be noted that the controller (21) has the same properties as the 3-STA presented in the previous subsection. The only difference is that the DIC does not necessitate the design of a sliding surface ( $\psi(e_1, e_2)$ ) as in the 3-STA. The principle to reject disturbances is the same, by adding an extra discontinuous state that nullifies the disturbance. It achieves convergence in finite-time via a continuous control signal and has a simpler form.

#### 3.2.1. Necessary conditions for the convergence of the DIC algorithm

The following homogeneous Lyapunov candidate function (24) [15] is considered for the finite-time convergence of the closed-loop system:

$$V(e) = w_1 |e_1|^{\frac{4}{3}} + w_2 |e_2|^2 + w_3 |e_3|^4 + w_{13} e_1 e_3 - w_{23} e_2 |e_3|^2. \quad (24)$$

This function (24) is homogeneous of degree 4, and is positive definite if coefficients ( $w_1, w_{13}, w_2, w_{23}, w_3$ ) and gains  $k_1, k_2, k_3$  are properly designed. This leads also to have a negative definite time derivative of the Lyapunov function [15].

$$\begin{aligned} \dot{V}(e) = & \frac{4}{3} w_1 [e_1] \frac{2}{3} e_2 - 2w_2 k_1 [e_1] \frac{1}{3} e_2 - 2w_2 k_2 |e_2|^{\frac{3}{2}} + 2w_2 e_2 e_3 \\ & - 4w_3 k_3 [e_1]^0 e_3^3 + w_{13} e_3 e_2 - w_{13} k_3 |e_1| + w_{23} k_1 [e_1]^{\frac{1}{3}} [e_3]^2 \\ & + w_{23} k_2 [e_2]^{\frac{1}{2}} [e_3]^2 - w_{23} |e_3|^3 + 2w_{23} k_3 [e_1]^0 e_2 |e_3|. \end{aligned} \quad (25)$$

The conditions that must be fulfilled for the Lyapunov function to be positive globally definite and for its derivative to be negative definite and that provide stability in finite-time of the system (9) are the following:

$$0 < \frac{3^3 w_{13}^4 w_2}{4^3 w_1^3} < 4w_2 w_3 - w_{23}^2, \quad (26)$$

$$w_1, w_2, w_{13} > 0.$$

$\dot{V}$  is negative definite for every Lipschitz disturbance if:

$$k_3, w_{23} > 0$$

and if there exist  $\alpha$  such that:

$$q_{12} = \left( 2w_2 k_1 - \frac{4}{3} w_1 \right),$$

$$\alpha < 2 \frac{w_2}{w_{23}} - \frac{1}{w_{23} k_2} \sqrt{\frac{32 |q_{12}|^3}{27 w_{13} (k_3 - \Delta)}}, \quad (27)$$

$$\phi(\alpha) < v(\alpha),$$

where

$$\begin{aligned} v(\alpha) & \triangleq \frac{1}{w_{23} k_2} \left( w_{23} - 4w_3 (k_3 + \Delta) - \sqrt{\tau} \right), \\ \tau & = \frac{4w_{23}^3 k_1^3 (2w_2 k_2 - w_{23} k_2 \alpha)^2}{27 w_{13} (k_3 - \Delta) (2w_2 k_2 - w_{23} \alpha)^2 - 32 |q_{12}|^3}. \end{aligned} \quad (28)$$

In this case, the Lyapunov function  $V$  and its derivative  $\dot{V}$  satisfy the following inequality [15]:

$$\dot{V} \leq -\kappa V^{\frac{3}{4}} \quad (29)$$

Based on Theorem 2 [29], finite-time convergence is guaranteed using the DIC controller.

## 4. Simulation results

In the interest of highlighting the operation of the proposed third-order super-twisting algorithms, it is discussed, in this section, results of simulation of trajectory tracking control task of the five-degrees-of-freedom upper limb exoskeleton robot with the application of the two algorithms introduced previously (3-STA and DIC). A comparison with the finite-time NTSMC controller [12] is achieved to evaluate the performance of proposed controllers. Passive rehabilitation simulations will be performed afterwards with the algorithm having the best efficiency.

### 4.1. Methodology

At first, the full dynamic model of the exoskeleton robot (9) is implemented in Matlab/Simulink. Information on the inertial constants of the robot and the gravitational constants are provided in [23] as well as the uncertainties affecting these physical elements.

Initial angular positions and velocities of the joints are chosen as:  $q(0) = [-\pi/4 \ -\pi/5 \ \pi/6 \ \pi/4 \ \pi/5]^T$  (rad) and  $\dot{q}(0) = [0 \ 0 \ 0 \ 0 \ 0]^T$  (rad/s) respectively.

Whereas the desired trajectories are defined by:

$$q_{d_j} = \left( \sin \left( t + n \frac{\pi}{5} \right) \right) \quad (30)$$

where  $j = 0, \dots, 5$  the joints number and  $n = n + 1$ ;  $n(0) = 0$ .

The disturbance vector  $\tau_{\text{dis}}$  is considered as:

$$\tau_{\text{dis}} = 0.15\dot{q} + 0.1q + [0.2\sin(3t) \ 0.1\cos(4t) \ 0.1\sin(3t) \ 0.1\cos(4t) \ 0.15\sin(4t)]^T. \quad (31)$$

When applying the method of design of the gains and parameters proposed in [15, 18], it happens that it is really hard to find a set of gains and parameters that satisfy all the necessary conditions (presented in the previous section) using the proposed Lyapunov functions due to the fact that there are too many nonlinear inequalities that must be satisfied and the fact that the exoskeleton system's model is complex, nonlinear, uncertain and coupled with five input torques. Therefore, it was not possible to find the set of parameters that would validate the stability demonstration.

The selected gains used for the 3-STA and DIC are shown in Table 1. Through simulations, it is possible to get an idea of the effect that each of the gains has on the controllers to have the best performance outcomes. The procedure was to choose first the gain  $k_3 > \Delta$  as  $k_3$  influences disturbance rejection, then adjust  $k_2$  and  $k_1$  accordingly which affects the speed of convergence and the position tracking precision respectively. On the other hand, gains of the NTSMC (in Table 2) are kept from the [12] to be able to make the comparison after.

Table 1.

Parameters of the 3-STA and DIC controllers

	3-STA	DIC
$k_1$	[5.5 10.5 20.5 20.1 10.5]	[25.5 23.2 28.5 37.3 23.6]
$k_2$	[1.7 1.7 1.7 5.5 1.7]	[3.2 3.2 20.2 16.2 3.2]
$k_3$	[10.2 10.2 20.2 5.2 10.2]	[2.02 24.8 25.3 28.2 14.7]

Table 2.

Parameters of the NSTMC control [12]

Sliding surface gains	controller gains
$\rho = [0.5 \ 0.5 \ 0.5 \ 0.5 \ 0.5]$	$k_1 = [1 \ 1 \ 1 \ 1 \ 1]$
	$k_2 = [0.01 \ 0.01 \ 0.01 \ 0.01 \ 0.01]$
	$\Omega_1 = 3/4, \Omega_2 = 5/4$

## 4.2. Analysis of obtained results

To assess the functioning of the proposed algorithms in terms of the efficiency of achieving the trajectory tracking control task, we will first consider the position error, as it is the only direct measurement that we obtain from the sensors in actuated joints. In Fig. 2 and Fig. 3 the trajectory tracking results as well as the

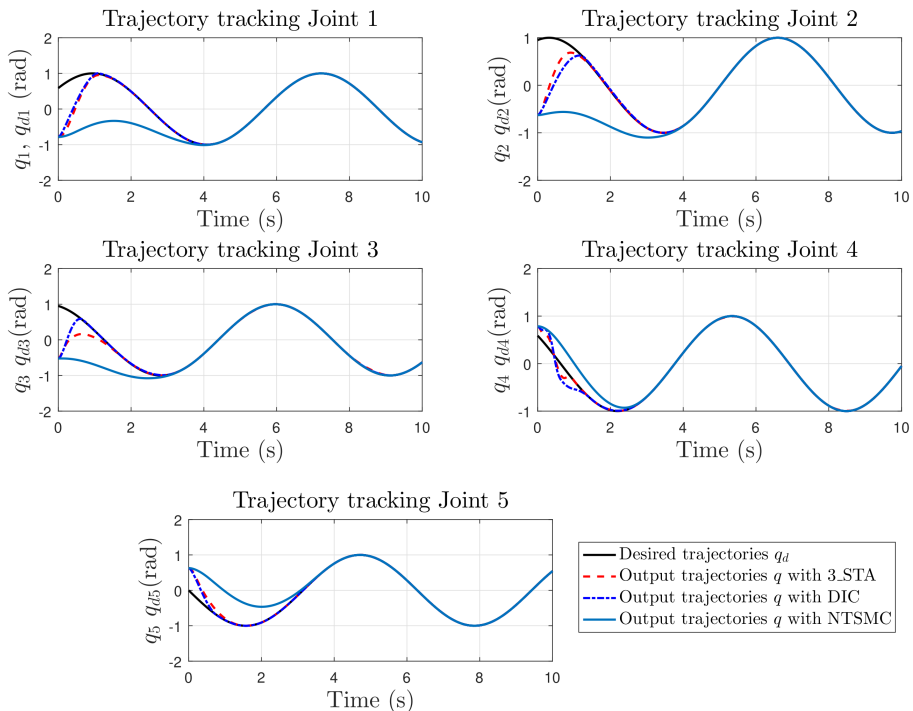


Fig. 2. Exoskeleton robot Trajectory tracking results

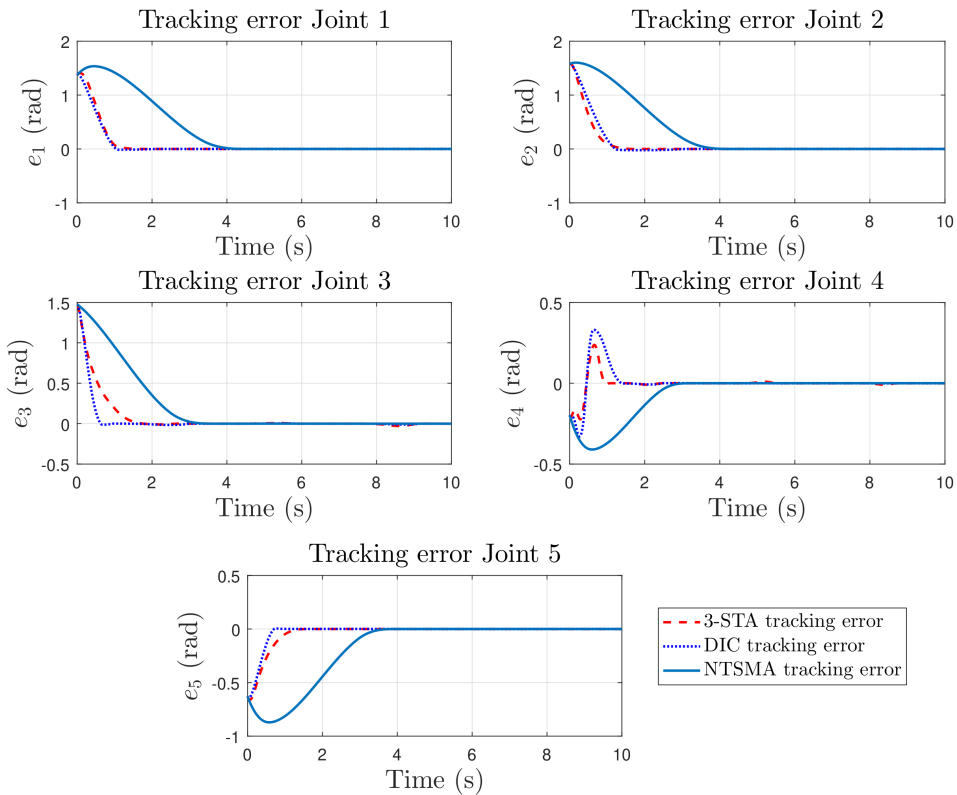


Fig. 3. Tracking error curves for the exoskeleton robot joints

corresponding errors for the five joints of the upper limb exoskeleton robot are illustrated.

After observing the obtained results for each of the exoskeleton joints with the two third-order sliding mode controllers and comparing them with the results of the NTSMC algorithm obtained in [12], it is quite clear that the efficiency of the system is significantly improved when controlled with the schemes proposed in this work, i.e., using the controllers founded on the third-order super twisting algorithm (3-STA) as well as the discontinuous integral controller (DIC). The responses obtained from the system are extremely fast, without overshoot and with great precision. On the other hand, comparing the performance of both controllers by sliding modes it can be said that in general the behavior is very similar, however the 3-STA produces faster responses.

The finite time settling times obtained for the responses of each joint of the exoskeleton robot deduced from Fig. 2 and Fig. 3 are listed in Table 3. These settling convergence times are consistent with the above discussion and the 3-STA controller offers the fastest convergence times to the desired trajectories despite of disturbances and uncertainties.

Table 3.

Settling time of the trajectory tracking

	Joint 1	Joint 2	Joint 3	Joint 4	Joint 5
3-STA	<b>1.517 s</b>	<b>1.617 s</b>	<b>2.597 s</b>	<b>2.456 s</b>	<b>0.965 s</b>
DIC	1.981 s	3.073 s	2.967 s	2.479 s	1.514 s
NTSMC	4.181 s	4.238 s	3.278 s	3.004 s	3.781 s

Fig. 4 shows the control signals of the three controllers by continuous sliding mode algorithms. Something that must be commented on these graphs is the amplitude of the control. Fig. 4 illustrates that the signals produced by the 3-STA are a little softer and are less saturated than those produced by the DIC, so they inject less energy into the system. On the other hand, the NTSMC necessitate more energy to achieve the control task which is clearly observed on the plots. Table 4 shows the maximum values taken by the control signals. It is noticed that much power is required by the first two joints with the three controllers since they are joints of the shoulder movement with are associated to more powerful motors.

Another comparative metric that allows us to give some conclusions about the performance of each algorithm is the Root Mean Square Error ( $\epsilon$ ) defined in

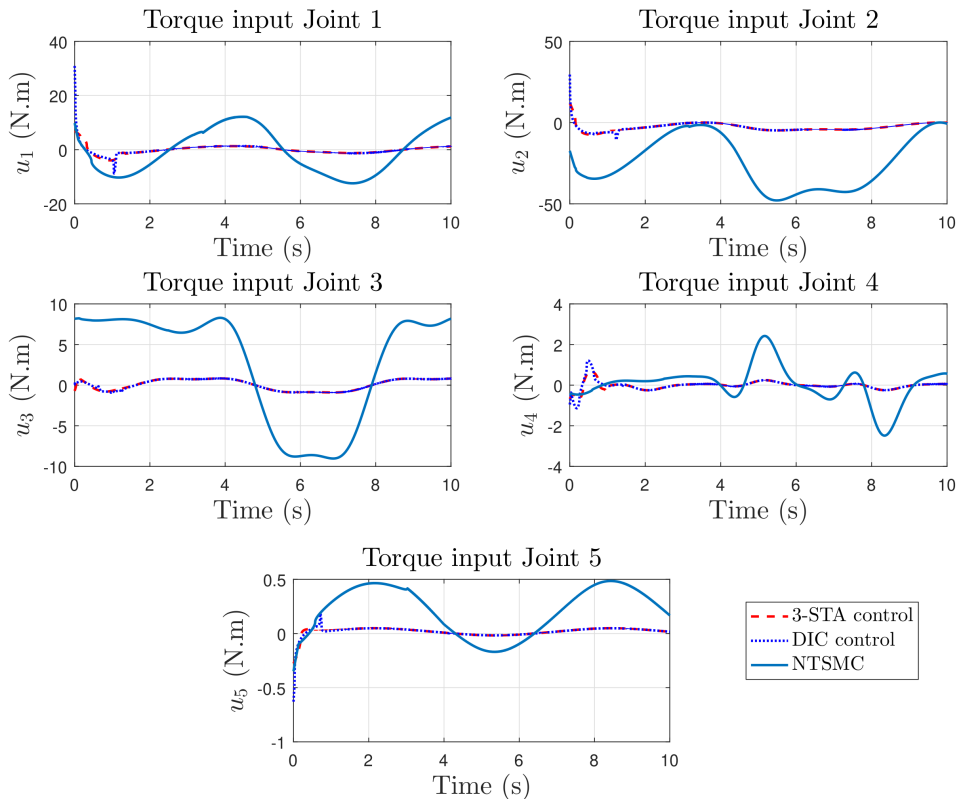


Fig. 4. Control input torques applied to the exoskeleton robot

Table 4.

Root mean square error and max torques of the joints of the robot

	$\epsilon$ (rad)			Max Torque (Nm)		
	3-STA	DIC	NTSMC	3-STA	DIC	NTSMC
Joint 1	0.2920	0.2634	0.6335	6.947	30.90	12.16
Joint 2	0.2812	0.3169	0.6127	11.92	29.54	47.9
Joint 3	0.2398	0.2077	0.4502	0.8974	0.8383	8.287
Joint 4	0.0514	0.0841	0.1455	0.6876	1.2094	2.422
Joint 5	0.1198	0.1039	0.3427	0.0490	0.1853	0.4854

(32). It is the measure of the accumulated error through each simulation. Table 4 enumerates the results of obtaining  $\epsilon$  for each controller and each joint of the exoskeleton robot.

$$\epsilon_i = \left[ \sum_{t=0}^{N \cdot \delta} (q_i(t) - q_{id}(t))^2 / N \right]^{1/2} \quad (32)$$

with  $i = 1, \dots, 5$  is the joint's number,  $N$  is the sample's number and  $\delta = 1$  ms is the sampling period.

It can be read from Table 4, that the best performance was the one that resulted from using the 3-STA, closely followed by DIC. The NTSMC did not show good results although it achieves the trajectory tracking task.

In theory, by increasing the order of the controller, the precision obtained in the sliding surface increases, but in turn, the complexity of the control law and the consumption of computational resources increases. On the other hand, in the physical implementation of controllers, the maximum achievable precision is restricted by the presence of imperfections (limited precision and speed in sensors and actuators, and time sampling, etc.) that do not allow the properties of sliding modes to be exploited to the maximum as an exact compensation for certain types of disturbances coupled to the control channel, convergence in finite-time and the increase in precision with respect to the increment of the order of the controller. Throughout this work, we observed that the higher order super twisting algorithms (3-STA, DIC) have simpler forms but complicated method to adjust gains using the proposed Lyapunov functions when it comes to complex systems. On the other hand, the NTSMC has a complex form of the control law which allows to achieve a continuous control, however, no method to adjust the gains is provided.

### 4.3. Simulation of passive rehabilitation exercises

A rehabilitation robot's primary function is to carry out therapeutic exercises prescribed by a physiotherapist. These exercises can be translated into specific trajectories for the exoskeleton robot to train the patients' limbs. Given that the 3-STA controller gave the best tracking results, we will simulate in this subsection two passive rehabilitation exercises of the shoulder and the elbow. The cubic polynomial

technique [30] is used to produce desirable trajectories for this purpose. The range of motion of the joints of the exoskeleton robot is given in Table 5 is used to design these trajectories. The initial conditions for angular positions and velocities, as well as the disturbance vector, remain unchanged.

Table 5.

Exoskeleton robot joint's range of motion[31]

Item	rotation range (deg)
Shoulder abduction/adduction	0 ~ 90
Shoulder flexion/extension	90 ~ -45
Elbow flexion/ extension	0 ~ 125
External / internal rotation	-90 ~ 90
Wrist flexion / extension	-75 ~ 75

Fig. 5 demonstrates a cooperative movement of the elbow (flexion/extension) and shoulder joint (internal/external rotation). The goal is to perform repetitive movement at the shoulder joint while keeping the elbow at 90 degrees. The first row of results (from top) shows the tracking results, while the second depicts the

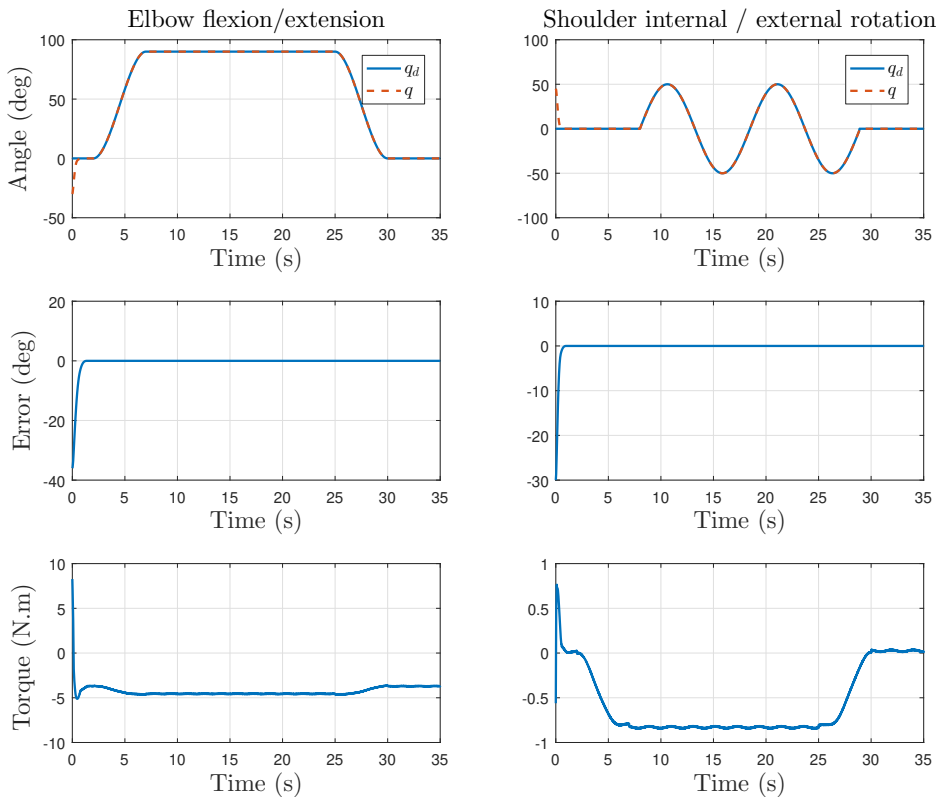


Fig. 5. Cooperative movement of the shoulder and the elbow joints



tracking error. The third row displays the input torques of the shoulder internal/external rotation and the elbow joints, respectively. It can be seen that the output trajectories (dotted line) nicely overlap with the desired trajectories (solid lines). The convergence time of the elbow joint is 1.329 s while that of the shoulder joint is 0.996 s which are acceptable times.

From multi-joint movement exercises, reaching movements are frequently employed and suggested. Fig. 6 depicts a repeating straight-ahead reaching movement in which the individual slides his hand softly over the surface of a table with the elbow's position starts at 90 degrees. This motion is similar to dusting a table because it requires simultaneous and repetitive rotation at the elbow (flexion/extension) and shoulder (flexion/extension). The first row depicts the tracking results while the second row the tracking error and finally the input torque is displayed in the third row. The settling convergence time of the elbow joint is 0.953 s and that of the shoulder joint is 1.365 s.

The obtained results Fig. 5 and Fig. 6 confirm the efficiency and robustness of 3-STA finite-time control strategy to achieve passive rehabilitation exercises. And thus should be adequate for the purpose of performing passive arm movement therapy.

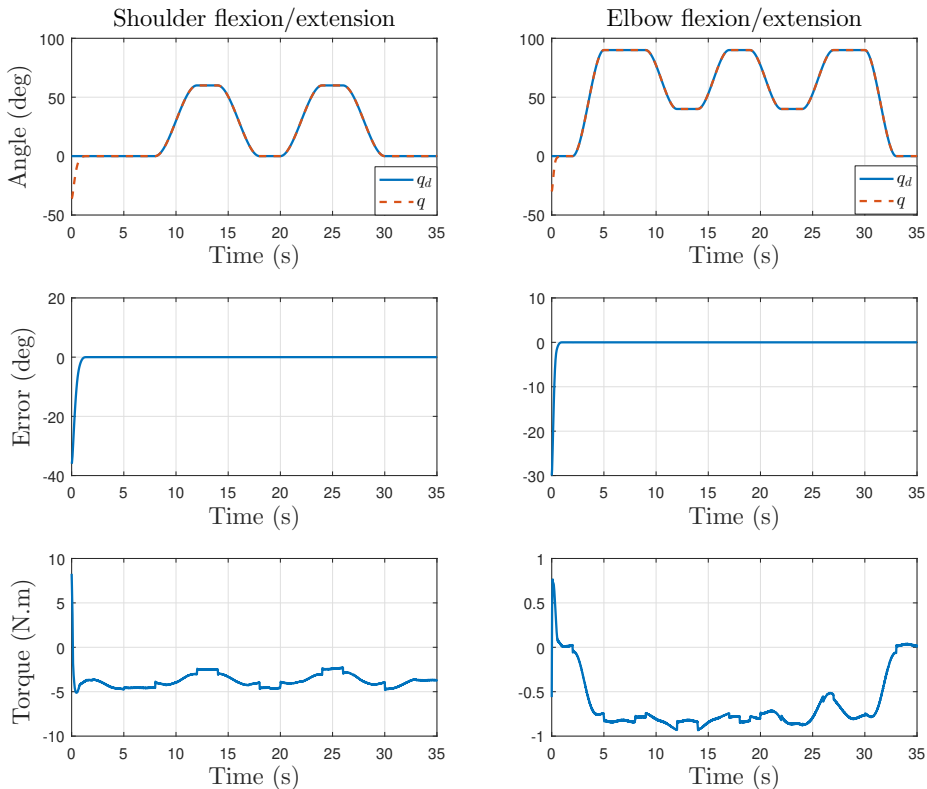


Fig. 6. Reaching movement of the shoulder and the elbow joints

## 5. Conclusion

In the present work, two new higher-order sliding mode control algorithms were examined for the first time to control a five-degrees-of-freedom upper limb exoskeleton robot, obtaining highly satisfactory results. The objective of trajectory tracking control task of the exoskeleton robot with these controllers was carried out with a fairly good performance and exceeding the results obtained with other control schemes found in the literature. In addition, a comparison was also accomplished between the presented control algorithms.

The 3-STA and the DIC algorithms that were used, are both controllers of third-order sliding modes, these have the property of bringing the system output and its first two derivatives to desired reference in finite-time. It is to implement these controllers directly to second order systems having a relative degree of two, such as the exoskeleton robot, that is, the design of a sliding variable is not required as in other sliding mode control algorithms. They produce continuous control system which alleviates the chattering problem and compensate for disturbances and uncertainties. Furthermore, through passive rehabilitation exercises simulations, it can be concluded that these algorithms should be adequate for the purpose of performing passive arm movement therapy. As an improvement of this work, an adaptation scheme for the gains would facilitate the design of gains and enhance the completion of the control tasks.

Manuscript received by Editorial Board, February 25, 2021;  
final version, August 27, 2021.

## References

- [1] N. Rehmat, J. Zuo, W. Meng, Q. Liu, S.Q. Xie, and H. Liang. Upper limb rehabilitation using robotic exoskeleton systems: a systematic review. *International Journal of Intelligent Robotics and Applications*, 2(3):283–295, 2018. doi: [10.1007/s41315-018-0064-8](https://doi.org/10.1007/s41315-018-0064-8).
- [2] A. Demofonti, G. Carpino, L. Zollo, and M.J. Johnson. Affordable robotics for upper limb stroke rehabilitation in developing countries: a systematic review. *IEEE Transactions on Medical Robotics and Bionics*, 3(1):11–20, 2021. doi: [10.1109/TMRB.2021.3054462](https://doi.org/10.1109/TMRB.2021.3054462).
- [3] A.C. Lo, P.D. Guarino, L.G. Richards, J.K. Haselkorn, G.F. Wittenberg, D.G. Federman, R.J. Ringer, et al. Robot-assisted therapy for long-term upper-limb impairment after stroke. *New England Journal of Medicine*, 362(19):1772–1783, 2010. doi: [10.1056/NEJMoa0911341](https://doi.org/10.1056/NEJMoa0911341).
- [4] P. Staubli, T. Nef, V. Klamroth-Marganska, and R. Riener. Effects of intensive arm training with the rehabilitation robot ARMin II in chronic stroke patients: four single-cases. *Journal of NeuroEngineering and Rehabilitation*, 6(1):46, 2009. doi: [10.1186/1743-0003-6-46](https://doi.org/10.1186/1743-0003-6-46).
- [5] A.S. Niyetkaliyev, S. Hussain, M.H. Ghayesh, and G. Alici. Review on design and control aspects of robotic shoulder rehabilitation orthoses. *IEEE Transactions on Human-Machine Systems*, 47(6):1134–1145, 2017. doi: [10.1109/THMS.2017.2700634](https://doi.org/10.1109/THMS.2017.2700634).
- [6] A. Michnik, J. Brandt, Z. Szczurek, M. Bachorz, Z. Paszenda, R. Michnik, J. Jurkojc, W. Ryckerski, and J. Janota. Rehabilitation robot prototypes developed by the ITAM Zabrze. *Archive of Mechanical Engineering*, 61(3):433–444, 2014. doi: [10.2478/meceng-2014-0024](https://doi.org/10.2478/meceng-2014-0024).

- [7] A. Gmerek. Mechanical and hardware architecture of the semi-exoskeleton arm rehabilitation robot. *Archive of Mechanical Engineering*, 60(4):557-574, 2013. doi: [10.2478/meceng-2013-0034](https://doi.org/10.2478/meceng-2013-0034).
- [8] I. Büsching, A. Sehle, J. Stürner, and J. Liepert. Using an upper extremity exoskeleton for semi-autonomous exercise during inpatient neurological rehabilitation – a pilot study. *Journal of NeuroEngineering and Rehabilitation*, 15(1):72, 2018. doi: [10.1186/s12984-018-0415-6](https://doi.org/10.1186/s12984-018-0415-6).
- [9] R. Fellag, T. Benyahia, M. Drias, M. Guiatni, and M. Hamerlain. Sliding mode control of a 5 dofs upper limb exoskeleton robot. In *2017 5th International Conference on Electrical Engineering – Boumerdes (ICEE-B)*, pages 1–6, Boumerdes, Algeria, 29-31 Oct. 2017. doi: [10.1109/ICEE-B.2017.8192098](https://doi.org/10.1109/ICEE-B.2017.8192098).
- [10] M.H. Rahman, M. Saad, J-P. Kenné, and P.S. Archambault. Control of an exoskeleton robot arm with sliding mode exponential reaching law. *International Journal of Control, Automation and Systems*, 11(1):92–104, 2013. doi: [10.1007/s12555-011-0135-1](https://doi.org/10.1007/s12555-011-0135-1).
- [11] T. Madani, B Daachi, and K. Djouani. Non-singular terminal sliding mode controller: Application to an actuated exoskeleton. *Mechatronics*, 33:136–145, 2016. doi: [10.1016/j.mechatronics.2015.10.012](https://doi.org/10.1016/j.mechatronics.2015.10.012).
- [12] A. Abooe, M.M. Arefi, F. Sedghi, and V. Abootalebi. Robust nonlinear control schemes for finite-time tracking objective of a 5-DOF robotic exoskeleton. *International Journal of Control*, 92(9):2178–2193, 2019. doi: [10.1080/00207179.2018.1430379](https://doi.org/10.1080/00207179.2018.1430379).
- [13] A. Riani, T. Madani, A. Benallegue, and K. Djouani. Adaptive integral terminal sliding mode control for upper-limb rehabilitation exoskeleton. *Control Engineering Practice*, 75:108–117, 2018. doi: [10.1016/j.conengprac.2018.02.013](https://doi.org/10.1016/j.conengprac.2018.02.013).
- [14] A. Jebri, T. Madani, and K. Djouani. Adaptive continuous integral-sliding-mode controller for wearable robots: Application to an upper limb exoskeleton. In *2019 IEEE 16th International Conference on Rehabilitation Robotics (ICORR)*, pages 766–771, Toronto, Canada, 24-28 June 2019. doi: [10.1109/ICORR.2019.8779431](https://doi.org/10.1109/ICORR.2019.8779431).
- [15] C.A. Zamora, J.A. Moreno, and S. Kamal. Control integral discontinuo para sistemas mecánicos. In *Congreso Nacional de Control Automático 2013*, pages 11–16. Ensenada, Mexico, Oct. 16-18, 2013. (in Spanish).
- [16] J.A. Moreno. Discontinuous integral control for systems with relative degree two. In: J. Clempner, W. Yu (eds.), *New Perspectives and Applications of Modern Control Theory*, pages 187–218. Springer, 2018. doi: [10.1007/978-3-319-62464-8\\_8](https://doi.org/10.1007/978-3-319-62464-8_8).
- [17] S. Kamal, J.A. Moreno, A. Chalanga, B. Bandyopadhyay, and L.M. Fridman. Continuous terminal sliding-mode controller. *Automatica*, 69:308–314, 2016. doi: [10.1016/j.automatica.2016.02.001](https://doi.org/10.1016/j.automatica.2016.02.001).
- [18] S. Kamal, A. Chalanga, J.A. Moreno, L. Fridman, and B. Bandyopadhyay. Higher order super-twisting algorithm. In: *2014 13th International Workshop on Variable Structure Systems (VSS)*, pages 1–5, Nantes, France, 29 June – 2 July 2014. doi: [10.1109/VSS.2014.6881129](https://doi.org/10.1109/VSS.2014.6881129).
- [19] A. Levant. Sliding order and sliding accuracy in sliding mode control. *International Journal of Control*, 58(6):1247–1263, 1993. doi: [10.1080/00207179308923053](https://doi.org/10.1080/00207179308923053).
- [20] J.A. Moreno and M. Osorio. Strict Lyapunov functions for the super-twisting algorithm. *IEEE Transactions on Automatic Control*, 57(4):1035–1040, 2012. doi: [10.1109/TAC.2012.2186179](https://doi.org/10.1109/TAC.2012.2186179).
- [21] J.A. Moreno and M. Osorio. A Lyapunov approach to second-order sliding mode controllers and observers. In: *2008 47th IEEE Conference on Decision and Control*, pages 2856–2861, Cancun, Mexico, 9-11 December 2008. doi: [10.1109/CDC.2008.4739356](https://doi.org/10.1109/CDC.2008.4739356).
- [22] R. Fellag, M. Hamerlain, S. Laghrouche, M. Guiatni, and N. Achour. Homogeneous finite time higher order sliding mode control applied to an upper limb exoskeleton robot. In *2019 6th International Conference on Control, Decision and Information Technologies (CoDIT)*, pages 355–360, Paris, France, 23-26 April 2019. doi: [10.1109/CoDIT.2019.8820676](https://doi.org/10.1109/CoDIT.2019.8820676).

- 
- [23] H-B. Kang and J-H. Wang. Adaptive control of 5 DOF upper-limb exoskeleton robot with improved safety. *ISA Transactions*, 52(6):844–852, 2013. doi: [10.1016/j.isatra.2013.05.003](https://doi.org/10.1016/j.isatra.2013.05.003).
- [24] H-B. Kang and J-H. Wang. Adaptive robust control of 5 DOF upper-limb exoskeleton robot. *International Journal of Control, Automation and Systems*, 13(3):733–741, 2015. doi: [10.1007/s12555-013-0389-x](https://doi.org/10.1007/s12555-013-0389-x).
- [25] B.O. Mushage, J.C. Chedjou, and K. Kyamakya. Fuzzy neural network and observer-based fault-tolerant adaptive nonlinear control of uncertain 5-DOF upper-limb exoskeleton robot for passive rehabilitation. *Nonlinear Dynamics*, 87(3):2021–2037, 2017. doi: [10.1007/s11071-016-3173-7](https://doi.org/10.1007/s11071-016-3173-7).
- [26] M.W. Spong and M. Vidyasagar. *Robot Dynamics and Control*. John Wiley & Sons, 2008.
- [27] A. Levant. Homogeneity approach to high-order sliding mode design. *Automatica*, 41(5):823–830, 2005. doi: [10.1016/j.automatica.2004.11.029](https://doi.org/10.1016/j.automatica.2004.11.029).
- [28] S. Kamal, A. Chalanga, V. Thorat, and B. Bandyopadhyay. A new family of continuous higher order sliding mode algorithm. In: *2015 10th Asian Control Conference (ASCC)*, pages 1–6, Kota Kinabalu, Malaysia, 31 May – 3 June 2015. doi: [10.1109/ASCC.2015.7244591](https://doi.org/10.1109/ASCC.2015.7244591).
- [29] S.P. Bhat and D.S. Bernstein. Finite-time stability of continuous autonomous systems. *SIAM Journal of Control and Optimization*, 38(3):751–766, 2000. doi: [10.1137/S0363012997321358](https://doi.org/10.1137/S0363012997321358).
- [30] J.J. Craig. *Introduction to Robotics: Mechanics and Control*, 3rd ed. Pearson Education International, 2009.
- [31] J-H. Wang, Z-B. Jiang, X-F. Wang, Y. Zhang, and D. Guo. Kinematics simulation of upper limb rehabilitant robot based on virtual reality techniques. In: *2011 2nd International Conference on Artificial Intelligence, Management Science and Electronic Commerce (AIMSEC)*, pages 6681–6683, Deng Feng, China, 8-10 August 2011. doi: [10.1109/AIMSEC.2011.6009874](https://doi.org/10.1109/AIMSEC.2011.6009874).